Chemistry and Physics of Lipids 157 (2009) 94–103

Contents lists available at ScienceDirect

Chemistry and Physics of Lipids

journal homepage: www.elsevier.com/locate/chemphyslip

Liposomes containing alkylated methotrexate analogues for phospholipase A_2 mediated tumor targeted drug delivery

Thomas Kaasgaard[a,b,c,*], Thomas L. Andresen[a,d], Simon S. Jensen[e], René O. Holte[a], Lotte T. Jensen[a], Kent Jørgensen[a]

[a] LiPlasome Pharma A/S, Department of Chemistry, Technical University of Denmark, DK-2800 Lyngby, Denmark
[b] MEMPHYS – Center for Biomembrane Physics, Physics Department, University of Southern Denmark, Campusvej 55, DK-5230 Odense M, Denmark
[c] Danish Technological Institute, Holbergsvej 10, DK-6000 Kolding, Denmark
[d] DTU Nanotech, Technical University of Denmark, 4000 Roskilde, Denmark
[e] Bioneer A/S, Kogle Allé 2, DK-2970 Hørsholm, Denmark

ARTICLE INFO

Article history:
Received 27 May 2008
Received in revised form
12 September 2008
Accepted 17 November 2008
Available online 27 November 2008

Keywords:
Methotrexate analogue
Phospholipase A_2
Drug delivery
Liposome
Tumor targeting
Synthesis

ABSTRACT

Two lipophilic methotrexate analogues have been synthesized and evaluated for cytotoxicity against KATO III and HT-29 human colon cancer cells. Both analogues contained a C_{16}-alkyl chain attached to the γ-carboxylic acid and one of the analogues had an additional benzyl group attached to the α-carboxylic acid. The cytotoxicity of the γ-alkylated compound towards KATO III (IC_{50} = 55 nM) and HT-29 (IC_{50} = 400 nM) cell lines, was unaffected by the alkylation, whereas the additional benzyl group on the α-carboxyl group made the compound nontoxic. The γ-derivative with promising cytotoxicity was incorporated into liposomes that were designed to be particularly susceptible to a liposome degrading enzyme, secretory phospholipase A_2 ($sPLA_2$), which is found in high concentrations in tumors of several different cancer types. Liposome incorporation was investigated by differential scanning calorimetry (DSC), and $sPLA_2$ hydrolysis was examined by fluorescence spectroscopy and high performance liquid chromatography (HPLC). The results showed that the methotrexate (MTX)-analogue could be incorporated into liposomes that were degradable by $sPLA_2$. However, the *in vitro* cytotoxicity of the MTX-liposomes against KATO III and HT-29 cancer cells was found to be independent of $sPLA_2$ hydrolysis, indicating that the alkylated MTX-analogue was available for cancer cell uptake even in the absence of liposome hydrolysis. Using a DSC based method for assessing the anchoring stability of alkylated compounds in liposomes, it was demonstrated that the MTX-analogue partitioned into the water phase and thereby became available for cell uptake. It was concluded that liposomes containing alkylated MTX-analogues show promise as a drug delivery system, although the MTX-analogue needs to be more tightly anchored to the liposomal carrier. Also, the developed DSC-assay for studying the anchoring stability of alkylated drugs will be a useful tool in the development of liposomal drug delivery systems.

© 2008 Elsevier Ireland Ltd. All rights reserved.

1. Introduction

Methotrexate (MTX) is an anticancer drug that has been used in the treatment of various cancer types for decades (Acute Leukemia Group B, 1965). It is an antimetabolite that inhibits dihydrofolate reductase (DHFR), which is an enzyme involved in the biosynthetic pathway of nucleotides and MTX is therefore highly toxic to rapidly dividing cancer cells (Subramanian and Kaufman, 1978; Bertino et al., 1996). However, MTX has a narrow therapeutic index, and its clinical use is hampered by severe dose-limiting side effects, as well as intrinsic and acquired drug resistance mechanisms of cancer cells (Frei et al., 1984; Bertino et al., 1996; Mauritz et al., 2002; Serra et al., 2004).

Various approaches have been attempted to overcome drug resistance and improve the therapeutic index of MTX. Synthesis of MTX-analogues having a molecular structure that is slightly different from that of the parent molecule is one approach to overcome drug resistance that has been employed for several years (Montgomery et al., 1979). The main strategy is to make alterations to the MTX-molecule that renders the analogue insensitive to, or able to bypass drug resistance mechanisms, and yet retain the cytotoxic activity towards the DHFR target enzyme. An exhaustive number of publications report on the effects that different alterations to the MTX-molecule have on DHFR inhibition and cytotoxic potency of the synthesized analogues (Piper et al., 1982a; Rosowsky et al., 1983, 1988a,b). Such studies have shown that particularly the γ-carboxyl group (Rosowsky et al., 1981, 1986), and to a lesser

* Corresponding author at: Danish Technological Institute, Holbergsvej 10, DK-6000 Kolding, Denmark. Fax: +45 72201919.
E-mail address: thomas.kaasgaard@teknologisk.dk (T. Kaasgaard).

0009-3084/$ – see front matter © 2008 Elsevier Ireland Ltd. All rights reserved.
doi:10.1016/j.chemphyslip.2008.11.005

extent the α-carboxyl (Piper et al., 1982b; Rosowsky et al., 1984), are amenable to derivatization without the loss of cytotoxicity.

A different approach to improve the therapeutic index of MTX is the use of an effective drug delivery system that is capable of tumor specific targeting. In a study by Pignatello et al. (2003), lipo-amino acids were conjugated to both of the carboxyl groups of the glutamate moiety, and the resulting lipophilic conjugates were incorporated into liposomes. Apart from enabling liposomal drug delivery, the increased lipophilicity of the synthesized MTX-conjugates also aimed to overcome impaired active transport drug resistance, by increasing the passive diffusion of drugs through the plasma membrane of cancer cells. In another study, MTX as well as another anticancer agent, docosahexanoic acid (DHA), were conjugated to the same phosphatidylcholine headgroup (Zerouga et al., 2002). When incorporated into liposomes, the synthesized MTX-DHA construct was reported to be hydrolyzed by snake venom phospholipase A_2 (snake-PLA_2). Snake-PLA_2 is a small water soluble lipid degrading enzyme that cleaves phospholipids at the liposome interface resulting in the formation of fatty acid and lysolipid hydrolysis products. It is structurally and functionally similar to human secretory phospholipase A_2 ($sPLA_2$), which is of particular interest in the context of liposomal drug delivery, as human secretory phospholipases are overexpressed in many types of solid tumors (Abe et al., 1997; Graff et al., 2001; Jiang et al., 2002).

The aim of the present study was to synthesize lipophilic derivatives of MTX for incorporation into liposomal drug carriers, which are made particularly susceptible to hydrolysis by human $sPLA_2$, whereby a tumor specific release of the MTX-analogue is expected. We have synthesized two lipophilic MTX-ester derivatives that each contain a C_{16}-alkane chain attached to the γ-carboxylic acid, and in one case also a benzyl group attached to the α-carboxylic acid. The cytotoxicity of both MTX-analogues was evaluated against KATO III and HT-29 cancer cell lines. These cell lines were chosen because KATO III cells secrete $sPLA_2$, whereas HT-29 cells do not. They were therefore suitable for testing the objective of $sPLA_2$ dependent release of the alkylated MTX-analogues from a liposomal formulation. The MTX-ester derivatives were incorporated into DPPC/DPPG/DPPE-PEG_{2000} liposomes and the MTX liposomal formulations were characterized by differential scanning calorimetry (DSC). The liposomal carrier was chosen as a composition expected to be particularly susceptible to $sPLA_2$ hydrolysis, as the phase transition temperature is close to physiological temperature, and it is known that $sPLA_2$ activity is high close to the phase transition, while the incorporation of DPPG introduces a negative charge on the liposomes, which is required for $sPLA_2$ to be active (Buckland and Wilton, 2000; Leidy et al., 2006). In contrast, more commonly employed liposomal carriers, have been shown not to be susceptible to $sPLA_2$ hydrolysis (Andresen et al., 2005). It was decided to attach a C_{16}-alkyl chain to MTX in order for the alkyl chain length to match the chain length of the liposomal carrier lipids. The susceptibility of the liposomal formulations towards PLA_2-mediated hydrolysis was studied by fluorescence spectroscopy and HPLC, using both human type and snake venom PLA_2 isoforms. Subsequently, the liposomal MTX-formulations were tested for cytotoxicity in $sPLA_2$-expressing KATO III cells as well as non-expressing HT-29 cancer cell lines. Finally, the anchoring stability of the MTX-ester in the drug delivery liposomes was characterized by means of a DSC method where liposomes are used as sensors for detecting MTX-ester dissociation from the drug delivery liposomes.

2. Materials and methods

The lipids 1,2-dimyristoyl-*sn*-glycero-3-phosphatidylcholine (DMPC), 1,2-dipalmitoyl-*sn*-glycero-3-phosphatidylcholine (DPPC), 1,2-dipalmitoyl-*sn*-glycero-3-phosphatidylglycerol (DPPG), 1,2-dipalmitoyl-*sn*-glycero-3-phosphatidylethanolamine-*N*-[poly(ethylene glycol)-2000] (DPPE-PEG_{2000}), were obtained from Avanti Polar Lipids, Inc. (Alabaster, AL, USA) and used without further purification. Boc-L-glutamic acid α-benzyl ester, 4-[*N*-(2,4-diamino-6-pteridinylmethyl)-*N*-methylamino] benzoic acid (PMAB), and all other chemicals used in the synthesis of the MTX-esters were purchased from Sigma–Aldrich and used without purification. Methotrexate-γ-hexadecyl ester (C_{16}-MTX-ester) and methotrexate-α-benzyl-γ-hexadecyl ester (C_{16}-MTX-benzyl-ester) was synthesized in our own laboratory as described below.

2.1. Synthesis of MTX-esters

The MTX-esters were synthesized from α-benzyl-BOC-protected glutamic acid as described in Scheme 1. Briefly, *N-t*-BOC-L-glutamic acid α-benzyl ester was coupled with hexadecyl alcohol using standard DCC, DMAP reaction conditions. The BOC protection group was hereafter removed by TFA and the resulting intermediate was used without purification in the coupling to PMAB. The desired C_{16}-MTX-benzyl-ester was hereby obtained in 61% overall yield. It was furthermore possible to remove the benzyl group using boron trichloride without destroying the pteridine, resulting in C_{16}-MTX-ester in 48% overall yield from the protected glutamic acid. Experimental is provided below.

Synthesis of N-t-BOC-α-benzyl-L-glutamic acid γ-hexadecyl ester. DCC 1 M in DCM (5.34 ml) was added to a solution of *N-t*-BOC-α-benzyl-L-Glutamic acid (1.80 g, 5.34 mmol), *n*-hexadecyl alcohol (863 mg, 3.56 mmol) and DMAP (87 mg, 0.712 mmol) in dry DCM (30 ml) under N_2. The reaction mixture was stirred at room

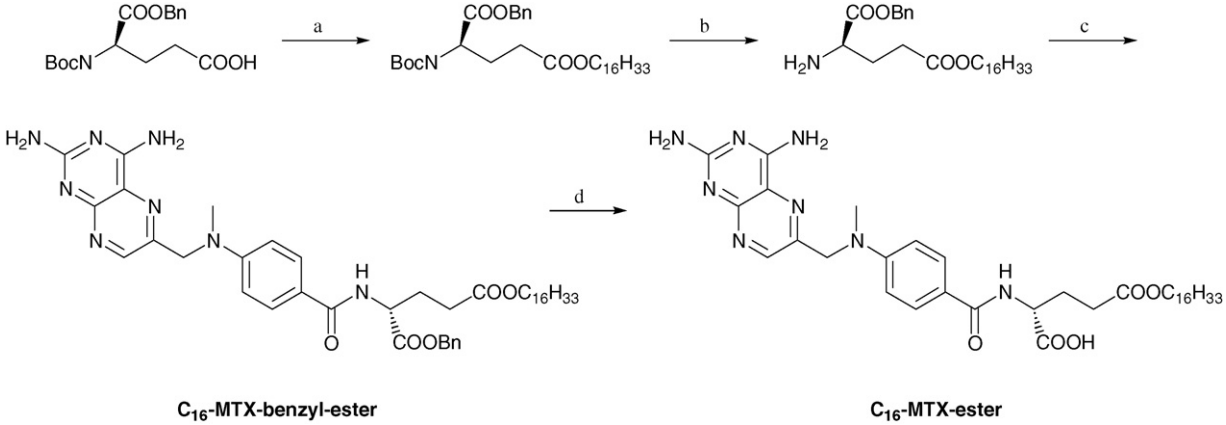

Scheme 1. Synthesis of C_{16}-MTX-ester and C_{16}-MTX-benzyl-ester. (a) $C_{16}H_{33}OH$, DMAP, DCC, DCM, rt, 16 h. (b) TFA, DCM, 0 °C, 30 min. (c) PMAB, EDCl, pyridine, rt, 12 h. (d) BCl_3, $CHCl_3$, from −20 °C to rt, 30 min.

temperature overnight, after which it was filtered and concentrated. The crude product was purified by flash chromatography (elution with hexane/DCM/diethyl ether 30:12:3 followed by 20:12:3) to give 1.98 g (99%) of the desired product as a white solid. R_F = 0.13 hexane/DCM/diethyl ether 30:12:3, R_F = 0.33 hexane/DCM/diethyl ether 20:12:3. ^{1}H-NMR (500 MHz, $CDCl_3$) δ = 7.36 (m, 5H), 5.18 (AB, J = 12.3 Hz, 2H), 5.11 (m, 0.5H), 4.38 (m, 0.5H), 4.05 (t, J = 6.8 Hz, 2H), 2.37 (m, 2H), 2.18 (m, 1H), 1.97 (m, 1H), 1.61 (k, J = 6.7 Hz, 2H), 1.44 (s, 9H), 1.27 (br. s, 26H), 0.89 (t, J = 7.0, 3H). ^{13}C-NMR (125 MHz, $CDCl_3$): δ = 172.7, 172.0, 155.3, 135.3, 128.6, 128.4, 128.2, 80.0, 67.1, 64.9, 53.0, 31.9, 30.3, 29.8, 29.6, 29.6, 29.5, 29.3, 29.2, 28.6, 28.3, 27.7, 25.9, 22.7, 14.1.

Synthesis of MTX-α-benzyl-γ-hexadecyl ester. *N-t*-BOC-α-benzyl-L-glutamic acid γ-hexadecyl ester (540 mg, 0.961 mmol) in dry DCM (6 ml) was placed in an ice bath for 10 min after which TFA (6 ml) was added. The solution was stirred 30 min and the solvent was removed under reduced pressure using toluene as co-evaporant. The crude product was redissolved in toluene (100 ml) and washed with 1 M HCl (2 × 10 ml), brine (10 ml), sat. $NaHCO_3$ (2 × 10 ml) and H_2O (2 × 10 ml). The organic layer was concentrated to give 450 mg of crude product. The crude product in pyridine (10 ml) was added to a solution of PMAP (200 mg, 0.481 mmol) in dry pyridine (20 ml) under N_2, followed by addition of EDCl (461 mg, 2.40 mmol). The yellow reaction mixture was stirred at room temperature in the dark for 12 h. The mixture was concentrated and redissolved in toluene (200 ml) and washed with brine (2 × 20 ml) and H_2O (2 × 20 ml). The solution was concentrated and purified by flash chromatography (5% MeOH in DCM) to give 232 mg (62%) of the desired product as a yellow solid. R_F = 0.30 10% MeOH in DCM. Anal.Calcd for $C_{43}H_{60}N_8O_5{\cdot}H_2O$: C 65.62, H 7.94, N 14.24; Found: C 65.81, H 7.85, N 14.18. ^{1}H-NMR (500 MHz, $CDCl_3$) δ = 8.60 (s, 1H), 7.70 (d, J = 8.5 Hz, 2H), 7.33 (m, 5H), 7.01 (d, NH), 6.71 (d, J = 8.6 Hz, 2H), 5.18 (AB, J = 12.2 Hz, 2H), 4.84 (m, 1H), 4.69 (s, 2H), 3.99 (m, 2H), 3.13 (s, 3H), 2.42 (m, 2H), 2.29 (m, 1H), 2.14 (m, 1H), 1.54 (k, J = 6.6 Hz, 2H), 1.24 (br. s, 26H), 0.87 (t, J = 7.0, 3H). ^{13}C-NMR (125 MHz, $CDCl_3$): δ = 173.3, 172.3, 166.9, 162.9, 162.4, 155.2, 151.2, 149.6, 147.0, 135.3, 128.9, 128.6, 128.4, 128.2, 121.9, 121.6, 111.5, 67.2, 65.0, 55.9, 52.3, 39.1, 31.9, 30.5, 29.7, 29.6, 29.6, 29.5, 29.3, 29.2, 28.5, 27.3, 25.8, 22.6, 14.1.

Synthesis of MTX-γ-hexadecyl ester. A solution of MTX-α-benzyl-γ-hexadecyl ester (62 mg, 0.081 mmol) in $CHCl_3$ (5 ml) under N_2, was cooled to −20 °C in an acetone bath. BCl_3 1 M in DCM (1.61 ml) was added dropwise and the flask was removed from the cooling bath. The mixture was stirred 30 min at room temperature after which it was concentrated. Purification by flash chromatography (first, 10% MeOH in $CHCl_3$ then $CHCl_3$/MeOH/H_2O 80:20:1) to give 43 mg (79%) of the desired product. R_F = 0.20 $CHCl_3$/MeOH/H_2O 80:20:1. ^{1}H-NMR (500 MHz, D_5-pyridine) δ = 8.93 (d, NH), 8.71 (s, 1H), 8.25 (d, J = 8.8 Hz, 2H), 6.86 (d, J = 8.8 Hz, 2H), 5.39 (m, 1H), 4.67 (s, 2H), 4.09 (t, J = 6.7 Hz, 2H), 2.98 (s, 3H), 2.82 (m, 3H), 2.56 (m, 1H), 1.53 (k, J = 7.0 Hz, 2H), 1.24 (br. s, 26H), 0.84 (t, J = 6.7, 3H). ^{13}C-NMR (125 MHz, $CDCl_3$): δ = 173.4, 167.9, 164.4, 164.3, 156.0, 151.8, 150.2, 149.6, 146.8, 129.8, 123.3, 122.9, 111.9, 64.8, 56.0, 53.5, 39.0, 32.2, 31.6, 30.0, 30.0, 29.0, 28.3, 26.2, 23.0, 14.3.

2.2. Preparation of liposomes

Stock solutions of DPPC and DPPE-PEG_{2000} were made in $CHCl_3$:CH_3OH 1:1 (v/v), whereas DPPG was in pure $CHCl_3$, and C_{16}-MTX was made in EtOH. Appropriate amounts of the stock solutions were mixed in a test tube, and the solvent evaporated using a gentle stream of nitrogen, followed by drying at low pressure overnight. The dry lipid mixtures were suspended in phosphate buffered saline buffer (PBS, without calcium, magnesium, and sodiumbicarbonate, GIBCO, Invitrogen, United Kingdom) and placed in a 51 °C water bath for at least 60 min. In the case of pure DMPC liposomes, DMPC was hydrated directly in PBS without prior evaporation from $CHCl_3$:CH_3OH. During the 60 min hydration period at 51 °C the lipid suspension was vigorously shaken every 15 min, producing multilamellar vesicles (MLVs). Subsequently, to create large unilamellar vesicles (LUVs), the MLV lipid suspensions were extruded (Avanti mini-extruder, Avanti Polar Lipids, Alabama, USA) ten times through a 0.1 μm polycarbonate filter (Nayar et al., 1989). MLV's were used in all DSC measurements because of the sharper phase transition produced by MLV's, while LUV's were used in all other measurements.

2.3. DSC-measurements

Differential scanning calorimetry (DSC) measurements were made using a MicroCal MC-2 calorimeter (Microcal Inc., Massachusetts, USA) at a scan rate of 30 °C/h. The concentrations of the MTX-ester containing liposomes were 3 mM, which was the total concentration of DPPC, DPPE-PEG_{2000}, C_{16}-MTX-ester and free MTX. For the measurements on anchoring stability (Figs. 9 and 10), 6 mM MLV suspension of the MTX formulation was mixed with a 6 mM MLV suspension of pure DMPC vesicles at a 1:1 ratio, giving 3 mM concentrations of each type of liposomes. The mixture was transferred to the calorimeter and a DSC scan recorded from 5 to 37 °C (scan 1). The sample was then incubated at 37 °C for 6 h and a second scan recorded (scan 2). Appropriate baselines were subtracted from the DSC curves.

2.4. PLA_2-hydrolysis measurements

The PLA_2 hydrolysis of unilamellar DPPC/DPPG/DPPE-PEG_{2000}/C_{16}-MTX (45:45:5:5) lipid vesicle suspensions (LUV's) was monitored by following the intrinsic tryptophan fluorescence emitted at 340 nm upon excitation at 285 nm. In addition, the 90° light scattering at 285 nm was measured, which is sensitive to changes in the lipid vesicles that results from the hydrolysis (Hønger et al., 1996). Fluorescence measurements were recorded using an SLM DMX-1100 spectrofluorometer (SLM-Aminco, Rochester, NY). The lipid concentration was 150 μM in PBS and $CaCl_2$ was added to give a $CaCl_2$ concentration of 1 mM. The temperature was 37 °C. In the case of snake venom PLA_2 hydrolysis, PLA_2 purified from *Agkistrodon piscivorus piscivorus* (Maraganore et al., 1984) was used at a concentration of 150 nM. In the case of human $sPLA_2$ hydrolysis, 10 μL of human tear fluid, which contains high amounts of $sPLA_2$ (Qu and Lehrer, 1998), was added to 2.5 mL of the lipid vesicle suspension. Tear fluid was collected by exposing healthy human adult volunteers to freshly minced onions.

2.5. HPLC-measurements

HPLC measurements were performed using a Waters Millenium 2010 (Milford, MA) HPLC equipped with a waters 510 pump, a Waters 717 Plus Autosampler, and a PL-EMD evaporative light scattering mass detector from Polymer Laboratories (Cheshire, UK). A 5 μm Phenomenex (Torrance, CA) diol spherical column and a mixture of chloroform/methanol/water (73:23:3) as isocratic mobile phase was used. Concentrations that were three times higher than in the fluorescence measurements were used for the snake venom PLA_2 experiment (i.e. 450 μM lipid; 450 nM snake venom PLA_2). From this reaction mixture, 100 μL samples were retrieved at different times of the reaction and added to 1 mL of a chloroform/methanol/acetic acid/water (2:4:1:1) mixture to stop the enzyme hydrolysis. Salts were then extracted from the sample by shaking thoroughly with 1 mL water. From the organic phase, 50 μL was used for HPLC analysis. For the tear fluid PLA_2-experiment, the lipid and enzyme concentration were the same as in the fluorescence measurements. A 300 μL sample was

retrieved from the reaction mixture and added to 1 mL of a chloroform/methanol/acetic acid/water (2:4:1:1) mixture, and salts were extracted by shaking with 800 μL of water. The degree of hydrolysis was calculated from the reduction in unhydrolyzed DPPC lipids, based on the integrated signal from the light scattering mass detector.

2.6. Cytotoxic activity assays

The KATO III human gastric carcinoma cell line was purchased from the Japan Health Sciences Foundation (Tokyo, Japan). The HT-29 and COLO 205 human colon carcinoma cell lines were purchased from ATCC (Manassas, VA). KATO III were grown in RPMI 1640 medium supplemented with 10% heat-inactivated fetal calf serum (FCS), 2 mM L-glutamine and 1 mM sodium pyruvate in a humidified 5% CO_2 atmosphere at 37 °C. HT-29 were grown in McCOY's 5A and COLO 205 in RPMI medium supplemented with 10% FCS, 2 mM L-glutamine (all from Invitrogen, Carlsbad, CA). Cells were plated in 96-well plates at a density of 1×10^4 cells per well, 24 h prior to addition of test compounds. MTX was solubilized in 0.1 M NaOH, MTX-ester in EtOH, MTX-benzyl-ester in $CHCl_3$. MTX-liposomes were added to the cells in phosphate buffered saline (PBS). Test compounds or formulations were added at the indicated concentrations and incubated for 72 h (Fig. 2) or 26 h (Fig. 7). MTX-ester release from liposomes was evaluated without $sPLA_2$ by addition of fresh media, and with $sPLA_2$ by addition of conditioned media from COLO 205 cells grown for 24 h containing 50–60 ng/mL $sPLA_2$. KATO III cells secreted approximately 3 ng/ml $sPLA_2$ over a 72 h incubation period (Jensen et al., 2004). The specific $sPLA_2$ inhibitor LY311727 was added in order to evaluate the specificity of $sPLA_2$-dependent release in $sPLA_2$-expressing cells. The LY311727 inhibitor (kindly provided by Eli Lilly & Co., Indianapolis, IN) was dissolved in ethanol and added to a final concentration of 25 μM 15 min before the addition of liposomes in order to allow for optimal inhibition of the lipase. Cytotoxic activity was assessed using a standard 3-(4,5-dimethylthiazolyl)-2,5-diphenyltetrazolium bromide (MTT) assay (Carmichael et al., 1987) and expressed as cell survival compared to vehicle treated control cells. All studies were performed in triplicate.

3. Results

3.1. Cytotoxicity of the synthesized MTX-analogues

The molecular structures of the two synthesized MTX-analogues are shown in Fig. 1.

Both analogues as well as the parent MTX-compound were tested for cytotoxic activity against KATO III and HT-29 cancer cell lines, and expressed as cell survival as presented in Fig. 2. The results reveal that the cytotoxic activity of C_{16}-MTX-ester is comparable to MTX in both cell lines. In contrast, the benzyl-MTX-ester turned out to be non-toxic in the tested concentration range. The IC_{50}-values based on the survival curves are approximately 55 nM for free MTX and the C_{16}-MTX-ester in KATO III cells, and 400 nM in HT-29 cells.

3.2. Incorporation into liposomes

Because the benzyl-MTX-ester was found to be non-toxic, this analogue was not investigated any further. The C_{16}-MTX-ester on the other hand, proved to be a promising candidate for liposome based drug delivery. For this reason, the C_{16}-MTX-ester was incorporated into liposomes and analyzed by DSC. Fig. 3a shows DSC heating curves of multilamellar DPPC liposomes containing different amounts of C_{16}-MTX-ester. The DSC curve of pure DPPC displays a main phase transition at 41.6 °C and a pretransition at 35.6 °C, as expected for this lipid. When increasing concentrations of C_{16}-

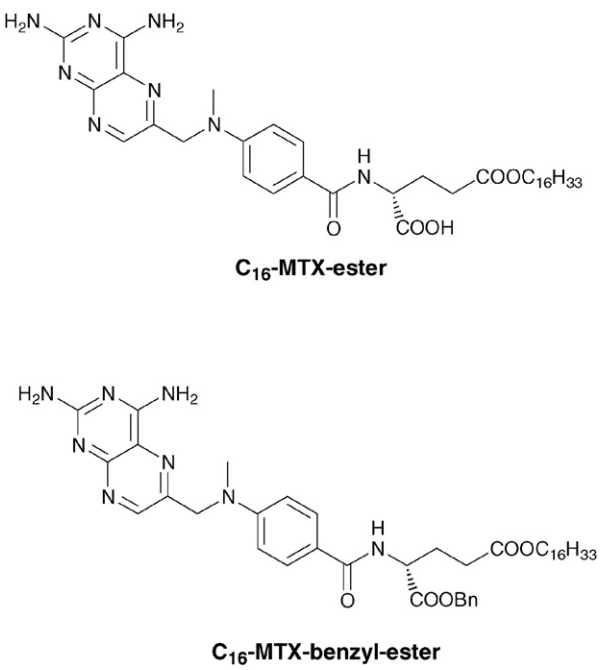

Fig. 1. Molecular structure of C_{16}-MTX-ester and C_{16}-MTX-benzyl-ester.

MTX-ester is incorporated, the main phase transition broadens and moves to lower temperatures, while the pretransition disappears as highlighted in Fig. 3b. At 25% C_{16}-MTX-ester, an additional broad peak appears in the 46–53 °C temperature range as shown in Fig. 3c. No additional peaks were observed at the lower concentrations of the MTX-analogue. As a control experiment, DSC scans of DPPC

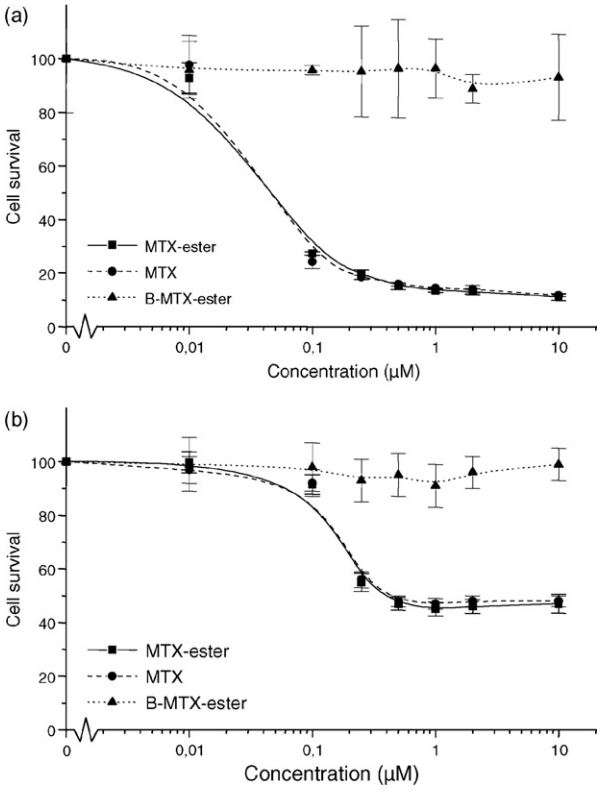

Fig. 2. Cytotoxicity of free MTX and MTX-ester and benzyl-MTX-ester after 72 h incubation in KATO III (a) and HT-29 (b) cancer cell lines. The cytotoxicity of the MTX-ester is comparable to that of free MTX. In contrast, benzyl-MTX-ester was nontoxic in both cell lines.

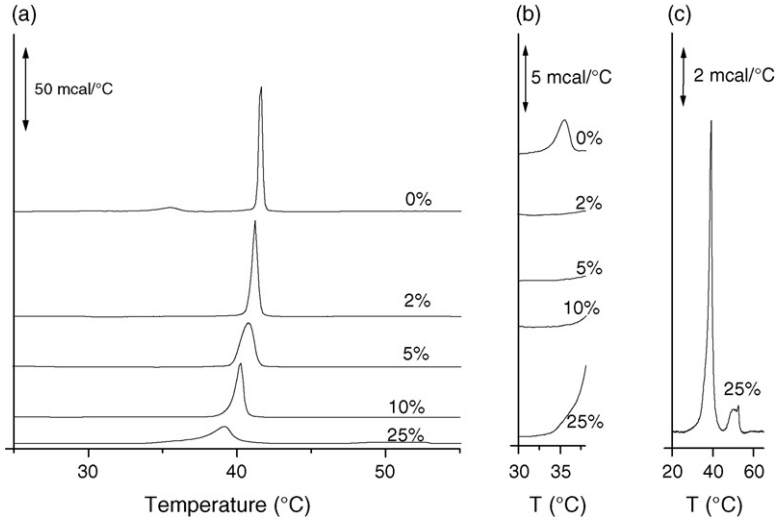

Fig. 3. DSC heating curves of DPPC multilamellar vesicles containing different concentrations of C_{16}-MTX-ester. (a) Main phase transition. (b) Magnification of the pretransition region, showing that the pretransition disappears when C_{16}-MTX-ester is incorporated. (c) Magnification of the DSC curve of the formulation containing 25% C_{16}-MTX-ester.

lipid vesicles in the presence of different concentrations of free MTX were recorded. In this experiment, the main phase transition temperature as well as the pretransition were virtually unaffected (data not shown) indicating a low partitioning of free MTX into the liposomal membrane.

The effects of free MTX and C_{16}-MTX-ester on the main phase transition temperature, T_m, and enthalpy, ΔH, are plotted in Fig. 4. The phase transition temperature decreases monotonously with increasing C_{16}-MTX-ester concentrations and is almost unchanged by free MTX (Fig. 4a). More intriguing are the enthalpy graphs shown in Fig. 4b, which show enthalpies that have been concentration normalized with respect to the DPPC lipid concentration. The molar enthalpy increases when C_{16}-MTX-ester is incorporated, while it decreases slightly with increasing concentrations of free MTX. Interestingly, the enthalpy increase caused by the C_{16}-MTX-ester is particularly pronounced when going from 0% to 2% of the MTX-analogue.

3.3. Hydrolysis by PLA_2

The aim of the present study was to make liposomal formulations that release the MTX-analogue as a result of $sPLA_2$-mediated hydrolysis in cancer tissue. Therefore, the susceptibility to PLA_2-mediated hydrolysis of the C_{16}-MTX-ester formulations was examined. Fig. 5a shows the hydrolysis of a DPPC/DPPG/DPPE-PEG_{2000}/C_{16}-MTX-ester (45:45:5:5) formulation by snake venom PLA_2. The lower curve is the fluorescence intensity of intrinsic tryptophan residues of PLA_2, and the upper curve is the light scattering, which is related to the morphology of the lipid vesicles. An increase in both the fluorescence and the light scattering intensity occurs at approximately 800 s, which is a clear indication that the lipid vesicles are being hydrolyzed by the PLA_2 enzyme, as has been demonstrated by a number of studies (Hønger et al., 1996; Høyrup et al., 2004). The same C_{16}-MTX-ester formulation was also subjected to hydrolysis by tear fluid $sPLA_2$, as shown in Fig. 5b. A steep increase in the light scattering occurs after a characteristic lag time of approximately 5000 s, indicating that the lipid vesicle formulation is also susceptible to hydrolysis by human $sPLA_2$ from tear fluid.

To further demonstrate that hydrolysis takes place, a parallel experiment was carried out, in which the lipid hydrolysis was monitored by HPLC. In order to get strong signals in the HPLC instrument, the snake-PLA_2 experiment shown in Fig. 6a was performed with three times higher lipid and enzyme concentrations than the concentrations used in the fluorescence/light scattering experiment.

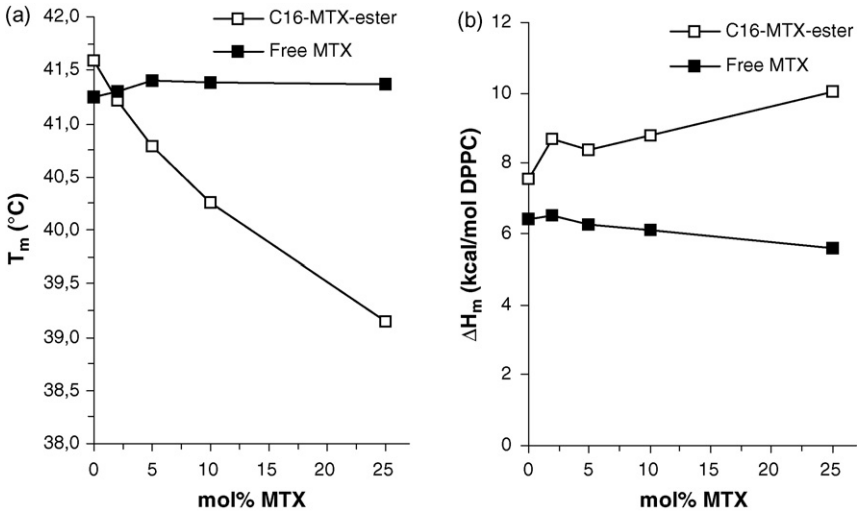

Fig. 4. The main phase transition temperature (a) and enthalpy (b) as a function of C_{16}-MTX-ester or free MTX content.

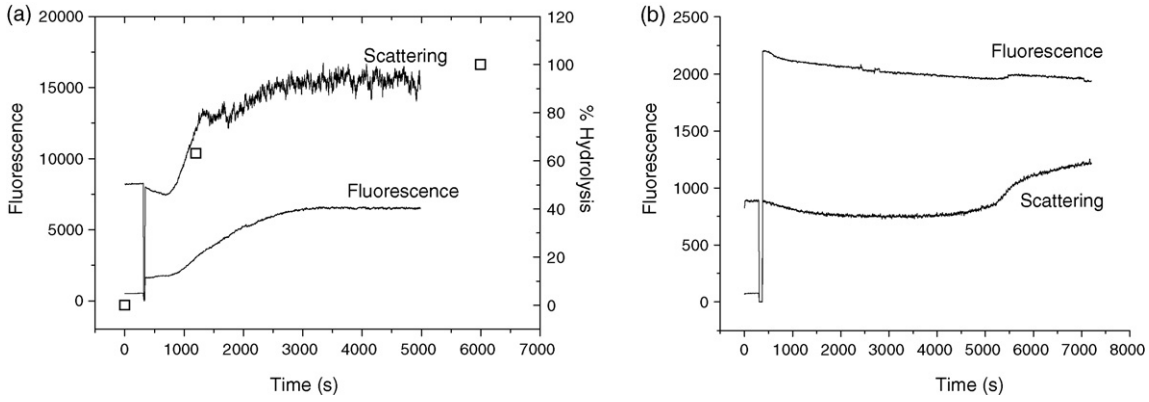

Fig. 5. Fluorescence spectroscopy measurements showing the hydrolysis of liposomes composed of DPPC/DPPG/PEG_{2000}/C_{16}-MTX-ester (45:45:5:5) by snake venom PLA_2 (a) and tear fluid PLA_2 (b).

In addition, blank liposomes without C_{16}-MTX-ester, but otherwise identical to the MTX-formulation were included in the measurements to examine the specific effects that MTX-ester might have on PLA_2 hydrolysis. The two peaks in the chromatogram correspond to unhydrolyzed DPPC that has a retention time between 6.5 and 7 min and palmitic acid that has a retention time of approximately 3.25 min and is one of the reaction products. The data demonstrate that DPPC is gradually degraded while palmitic acid is concomitantly being formed, and thus confirm the fluorescence data that the presence of MTX-ester does not inhibit PLA_2 mediated hydrolysis. In fact, it even appears that hydrolysis is slightly enhanced when MTX-ester is present in the liposomes. Based on the HPLC measurements, the extent of hydrolysis of the MTX-ester formulation was calculated at three different time points. The calculated hydrolysis percentages are plotted as open squares in Fig. 5a, and are in good accordance with the fluorescence and light scattering measurements. A quantitative HPLC analysis of tear fluid $sPLA_2$ catalyzed hydrolysis was not carried out because the higher lipid concentrations required for accurate HPLC detection would require correspondingly large amounts of tear fluid. However, Fig. 6b presents a HPLC chromatogram of a sample retrieved at the end of the fluorescence experiment in Fig. 5b. A distinct palmitic acid peak is seen at 3.25 min, providing qualitative confirmation that the C_{16}-MTX-ester liposomes are also susceptible to hydrolysis by human type $sPLA_2$.

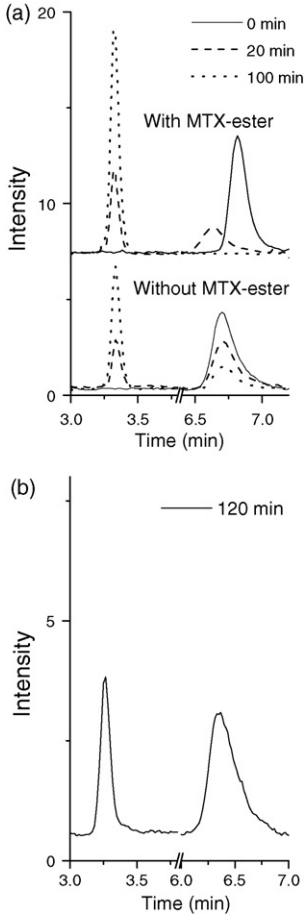

Fig. 6. HPLC chromatograms of DPPC/DPPG/PEG_{2000}/C_{16}-MTX-ester (45:45:5:5) at different times after the addition of snake venom PLA_2 (a) and tear fluid PLA_2 (b).

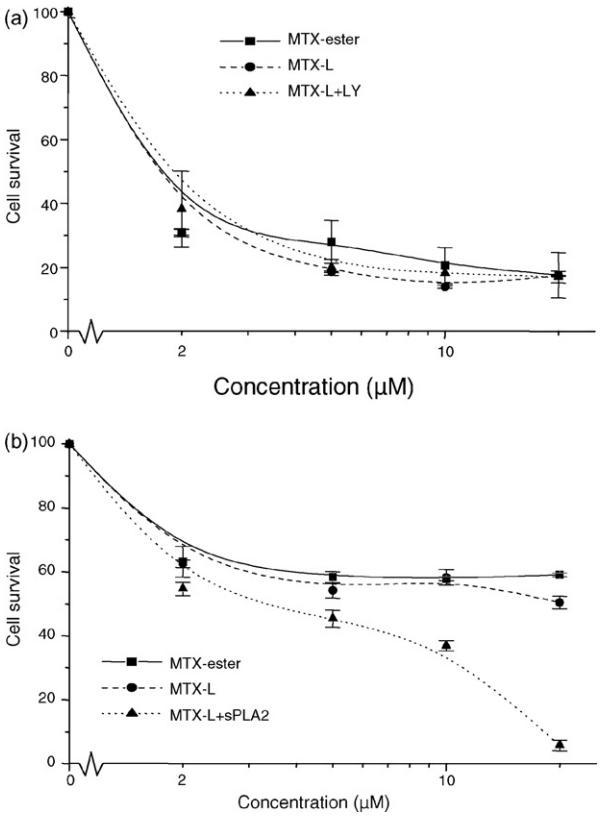

Fig. 7. Cytotoxic activity measured after 26 h in KATO III (a) and HT-29 (b) cancer cells of free C_{16}-MTX-ester (MTX-ester), DPPC/DPPG/PEG_{2000}/C_{16}-MTX-ester (45:45:5:5) liposomes (MTX-L), and MTX-L in the presence of the $sPLA_2$ inhibitor LY311727 inhibitor (MTX-L + Ly). For the non-$sPLA_2$-secreting HT-29 cell line, $sPLA_2$ was added from conditioned COLO 205 media (MTX-L + $sPLA_2$).

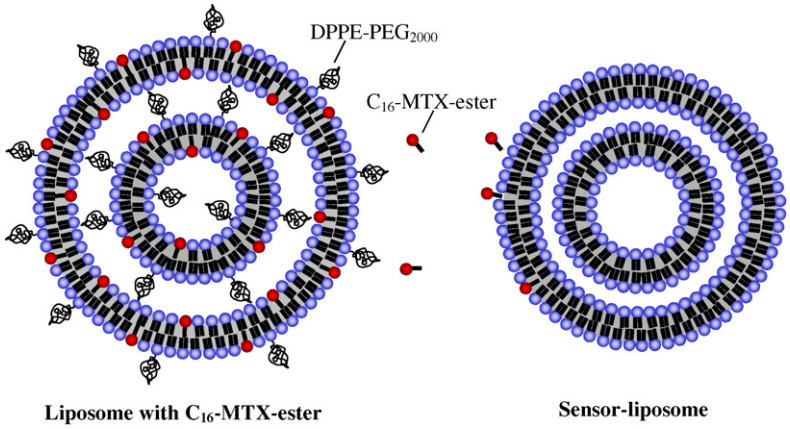

Fig. 8. Schematic illustration of a DSC-method for evaluating the anchoring stability of the MTX-ester in the liposomal formulation. The DPPC/DPPG/PEG_{2000}/C_{16}-MTX-ester liposomes are shown to the left and the C_{16}-MTX-ester is depicted in red. The extent of migration of MTX-ester from the liposomal formulation and into the sensor-liposomes is a measure of the anchoring stability of the MTX-ester, and can be evaluated from a DSC scan of the phase transition of the sensor liposomes. (For interpretation of the references to colour in this figure legend, the reader is referred to the web version of the article.)

3.4. PLA_2-dependent cytotoxicity

The abovementioned results indicate that it is possible to make a liposomal formulation of the highly toxic C_{16}-MTX-ester, and that such a formulation is degradable by $sPLA_2$. For this reason, a formulation consisting of DPPC/DPPG/DPPE-PEG_{2000}/C_{16}-MTX-ester (45:45:5:5) was prepared, and tested for $sPLA_2$ dependent cytotoxicity against KATO III and HT-29 cells (Fig. 7). KATO III cells secrete $sPLA_2$ whereas HT-29 cells do not. In the KATO III experiment, the cytotoxic effect of the liposome formulation was measured after 26 h of incubation and compared to the effect in the presence of the $sPLA_2$-inhibitor, LY311727, as well as to the free C_{16}-MTX-ester. No significant difference in cytotoxic activity was seen for these three treatment regimens (Fig. 7a). In the HT-29 experiment, $sPLA_2$ was added in the form of conditioned media from $sPLA_2$-secreting COLO 205 cells containing 50–60 ng/mL of $sPLA_2$. The results of the HT29 experiment show that MTX-liposomes and free MTX-ester are equally toxic in the absence of $sPLA_2$, whereas MTX-liposomes become the most toxic when $sPLA_2$ is added (Fig. 7b).

3.5. Anchoring stability

To test the stability of the MTX-ester in lipid vesicles of different compositions, a simple DSC method was developed. The method, which is depicted in Fig. 8, is based on co-incubating the MTX-ester liposomal formulation with pure DMPC liposomes and subsequently recording a DSC scan of the DMPC main phase transition. If MTX-ester is only loosely anchored in the formulation, it will dissociate from the liposomes and, in turn, partition into the DMPC vesicles. Upon migration of MTX-ester to the DMPC vesicles, the main phase transition peak will become progressively more perturbed by the presence of the MTX-ester, and the main phase transition of the DMPC liposomes can thus be used as a measure of the amount of MTX-ester which has migrated from the MTX-formulation to the DMPC vesicles. It is noted, that this experimental setup mimics the cytotoxicity measurements where MTX-ester containing liposomes are incubated with cancer cells.

Fig. 9a shows DSC scans of pure DMPC lipid vesicles co-incubated with a DPPC/DPPG/DPPE-PEG_{2000}/C_{16}-MTX-ester formulation. The uppermost DSC curve shows a scan of pure DMPC in the absence of the C_{16}-MTX-formulation, and the two other curves show DMPC vesicles at different times after mixing with the DPPC/DPPG/PEG_{2000}/C_{16}-MTX (45:45:5:5) formulation. The middle curve is the first scan obtained after the vesicles were mixed, and the lower curve was recorded after a 6-h incubation at 37 °C. It is evident that the presence of the MTX-ester formulation causes a significant and time dependent perturbation of the main phase transition of the DMPC liposomes. To ensure that the observed perturbations of the DMPC phase transition was due to the C_{16}-MTX-ester and not any of the lipid components, the lipid exchange between DMPC and DPPC/DPPG/PEG_{2000} (45:50:5) without the MTX-ester was examined (Fig. 9b). It is observed that the lipid components have a negligible effect on the DMPC phase transition, and it can therefore be concluded that the perturbation seen in Fig. 9a is due to C_{16}-MTX-ester.

Fig. 10 shows the effect of the negatively charged DPPG lipids on the anchoring stability of the MTX-ester in the liposome formulation. The top curve shows pure DMPC liposomes, and the following curves show DMPC liposomes after a 6-h co-incubation with MTX-ester formulations containing increasing amounts of DPPG. The results show that the DMPC phase transition becomes progressively more perturbed as the DPPG content is increased, indicating that the negatively charged DPPG decreases the anchoring stability of MTX-ester in the liposomal formulation.

4. Discussion

4.1. Cytotoxicity of the synthesized MTX-analogues

In this study, two MTX-ester analogues were synthesized and tested for cytotoxicity against two different cell lines. The derivative containing a C_{16} alkyl chain attached to the γ-carboxylic acid (Fig. 1a) was shown to be equally toxic as the parent MTX-molecule, whereas the attachment of an additional benzyl group to the α-carboxyl group (Fig. 1b) eliminated the toxicity of this MTX-analogue. This lends support to previous findings that the α-carboxylic acid is sensitive to derivatization (Piper et al., 1982b). However, some studies have shown that α-carboxyl ester derivatives retain activity (Rosowsky et al., 1984), and it was therefore conceivable that the benzyl-ester analogue tested in the present study would remain active as well. The main incentive for making alkylated MTX-derivatives was to incorporate the derivatives into $sPLA_2$-degradable liposomes that specifically release the drug at the tumor target site. It should be noted, however, that the increased hydrophobicity of the alkylated MTX-analogues may also increase the passive diffusion into cancer cells and thereby enhance the activity of the analogues towards resistant cell lines with lost or impaired active transport mechanisms (Frei et al., 1984; Pignatello et al., 2004). Although the cytotoxic activity graphs in Fig. 1 do not show indications of enhanced cytotoxicity, it is quite possible that

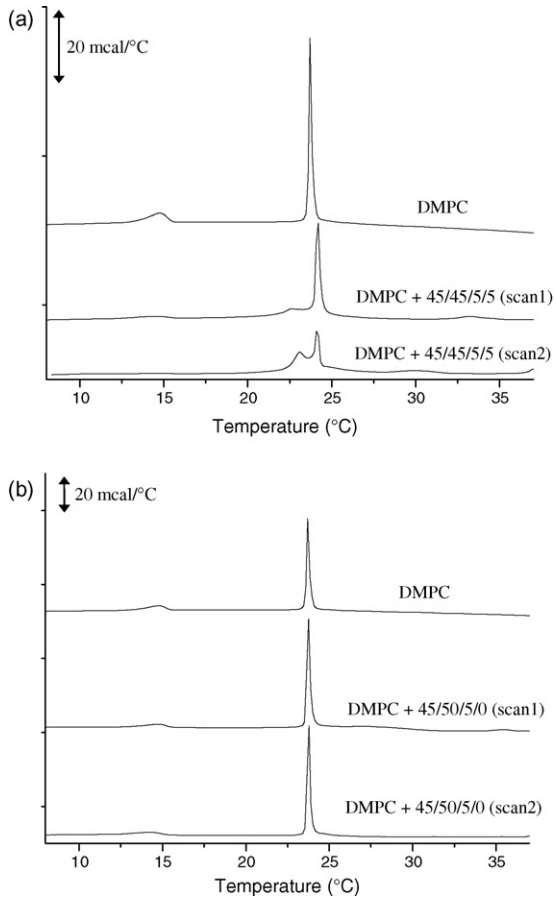

Fig. 9. (a) Stability of C_{16}-MTX-ester in the liposome formulation. The upper heat capacity curve shows a scan of pure DMPC liposomes in the absence of the C_{16}-MTX-formulation. The two other curves show DMPC liposomes co-incubated with a DPPC/DPPG/PEG_{2000}/C_{16}-MTX (45:45:5:5) formulation. The middle curve is the first scan after the vesicles were mixed, and the lower curve is the second scan, which was recorded after a 6-h incubation at 37 °C. Clearly, the DMPC main phase transition becomes perturbed as MTX-ester partitions into the DMPC liposomes. (b) To ensure that the observed perturbations of the DMPC phase transition was due to the C_{16}-MTX-ester and not any of the lipid components, the lipid exchange between DMPC and DPPC/DPPG/PEG_{2000}/C_{16}-MTX (45:50:5:0) was examined (i.e. without C_{16}-MTX-ester). The upper heat capacity curve shows a scan of pure DMPC liposomes. The two other curves show DMPC liposomes co-incubated with DPPC/DPPG/PEG_{2000}/C_{16}-MTX (45:50:5:0) liposomes. The middle curve is the first scan after the liposomes were mixed, and the lower curve is the second scan, which was recorded after a 6-h incubation at 37 °C. It is observed that the lipids have negligible effect on the DMPC phase transition.

enhanced activity would be observed *in vivo* or if the MTX-analogue was evaluated against resistant cell lines *in vitro*.

4.2. Liposome incorporation

The C_{16}-MTX-ester analogue that was equally active as the parent MTX-compound was next investigated for liposome incorporation by recording DSC scans of DPPC multilamellar vesicles (MLVs) containing different amounts of the MTX-ester (Figs. 3 and 4). The choice of pure DPPC MLVs for this experiment might seem surprising, considering that unilamellar vesicles consisting of a mixture of DPPC, DPPG, and DPPE-PEG_{2000} were used for the C_{16}-MTX-ester formulation in the PLA_2 hydrolysis and cytotoxic activity assays. However, pure DPPC MLVs are good probes for investigating the incorporation into liposomes, because they give rise to a sharp main phase transition peak that is very sensitive to changes in the lipid vesicle structure. In contrast, unilamellar DPPC/DPPG/DPPE-PEG_{2000} liposomes result in a fairly broad peak

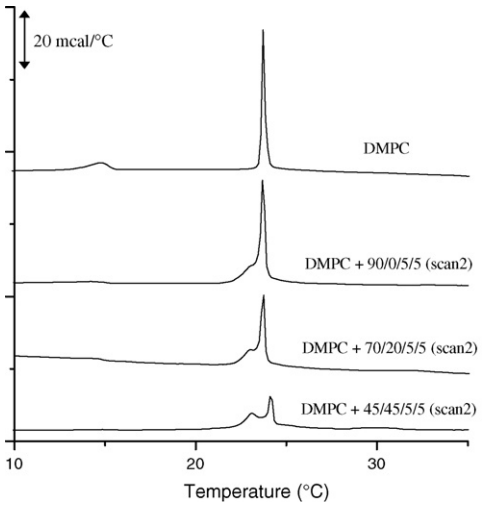

Fig. 10. Effect of DPPG content on the stability of C_{16}-MTX-ester in DPPC liposomes. The upper heat capacity curve shows a scan of pure DMPC in the absence of the C_{16}-MTX-formulation. The other three curves show DMPC liposomes co-incubated with DPPC/DPPG/PEG_{2000}/C_{16}-MTX formulations containing different amounts of DPPG, as indicated above each curve. All curves correspond to the second scan that was recorded after a 6-h incubation at 37 °C. The results indicate that the anchoring stability decreases as the DPPG content is increased.

reflecting phase coexistence and would not be as sensitive to the incorporation of small amounts of C_{16}-MTX-ester.

The DSC data presented in Figs. 3 and 4 strongly suggest that C_{16}-MTX-ester partitions into the DPPC liposomes. First of all, the concentration dependent and monotonous decrease in the main phase transition, as well as the disappearance of the pretransition indicate that C_{16}-MTX-ester is present in the liposomes and causes a slight perturbation of the lipid packing. Secondly, in contrast to free MTX, the molar enthalpy increases when the C_{16}-MTX-ester is incorporated (Fig. 4b). It is pointed out that the molar enthalpy presented in Fig. 4b is based on the DPPC concentration. Thus, the enthalpy increase that occurs when the C_{16}-MTX-ester is added implies that the C_{16}-MTX-ester alkyl chain is present in the apolar part of the liposomes and contributes to the chain melting enthalpy. The reason for the particularly large initial increase in the enthalpy that occurs from 0 to 2 mol% C_{16}-MTX-ester is unknown. However, the disappearance of the pretransition (Fig. 3b) may provide a plausible explanation why the enthalpy increases more dramatically at low C_{16}-MTX-ester contents. The pretransition is a low enthalpy transition that signifies the change from a gel phase to a ripple phase lipid bilayer, while the main phase transition signifies the change from a ripple phase to a fluid phase lipid bilayer (Tenchov, 1991; Biltonen and Lichtenberg, 1993). In the event that the C_{16}-MTX-ester prevents ripple phase formation, as Fig. 3b indicates, the lipid bilayer undergoes a gel to fluid phase transition without forming the intermediate ripple phase. In this case the new main phase transition enthalpy will be the sum of the pretransition and the main phase transition enthalpy, except for the perturbing effects of the MTX-analogue. The pretransition enthalpy calculated from the pure DPPC heat capacity curve in Fig. 3b is 1.55 kcal/mol. This value is similar in magnitude to the enthalpy jump observed in Fig. 4, and therefore lends weight to our hypothesis.

4.3. PLA_2-hydrolysis

Based on the DSC results, it was concluded that at least 10% of the C_{16}-MTX-ester can be incorporated into DPPC liposomes. Although we expect the lipid bilayer partitioning to be governed predominantly by the hydrophobic effect, the amount that can be incorporated into DPPC:DPPG:DPPE-PEG_{2000} liposomes is likely to

be different however. To be on the safe side, only 5% C_{16}-MTX-ester was therefore incorporated in the liposomal formulation, which apart from the MTX-ester was composed of 45 mol% DPPC, 45 mol% DPPG, and 5 mol% DPPE-PEG_{2000}. The high amount of DPPG was included in order to make the liposomes degradable to human $sPLA_2$, which is particularly active towards negatively charged liposomes (Buckland and Wilton, 2000; Buckland et al., 2000; Leidy et al., 2006).

The formulation was investigated for PLA_2-catalyzed hydrolysis by snake-PLA_2 as well as human $sPLA_2$, which tear fluid contains in high amounts (Qu and Lehrer, 1998). Snake-PLA_2 is structurally and functionally similar to human $sPLA_2$, and has the obvious advantage of being available in large quantities in a purified form. It does not possess the same preference for negatively charged lipids, but was nevertheless considered a good model enzyme. In particular, the fluorescence and HPLC experimental data obtained using snake-PLA_2, was a valuable reference for interpretation of the data obtained with human $sPLA_2$. The fluorescence and HPLC measurements shown in Figs. 5 and 6, strongly suggest that the liposomal formulation is hydrolyzable by both snake venom PLA_2 and human $sPLA_2$. The hydrolysis is particularly evident in the snake-PLA_2 experiments, which showed a dramatic change in the fluorescence intensity and light scattering in response to the PLA_2 hydrolysis (Fig. 5a), as well as a time dependent conversion of DPPC to its hydrolysis products (Fig. 6a). We were concerned that the presence of the C_{16}-MTX-ester could possibly impede the hydrolysis by perturbing the lipid bilayer structure or by inhibiting the enzyme. It was however interesting and promising to note that the opposite appeared to be the case and hydrolysis was enhanced when the C_{16}-MTX-ester was present in the liposomes. The human $sPLA_2$ experiments gave similar results, although hydrolysis was slower and the observed changes were less pronounced due to lower enzyme concentrations. Comparing the results to the snake venom data, however, leaves little doubt that the liposomal C_{16}-MTX-ester formulation is also being degraded by human $sPLA_2$.

4.4. PLA_2-dependent cytotoxicity

As the above findings have demonstrated that the C_{16}-MTX-ester is both equally toxic as free MTX, and amenable to incorporation into $sPLA_2$-degradable liposomes, the lipsomal formulation seemed a promising candidate for tumor targeted delivery of MTX-analogues to cancer tissue expressing $sPLA_2$. In Fig. 7a this hypothesis was tested using KATO III cells, which is one example of a $sPLA_2$-expressing cancer cell line. In this cell line, the cytotoxic activity of the liposomal formulation was similar to free C_{16}-MTX-ester, which is expected if the C_{16}-MTX-ester is being released into the aqueous media through $sPLA_2$-catalyzed liposome degradation. What was unexpected, however, was that the inhibition of $sPLA_2$ did not abolish the cytotoxic activity. This implies that C_{16}-MTX-ester is available for uptake into the KATO III cells even without the liposomes being degraded by $sPLA_2$. To further examine for $sPLA_2$ dependent cytotoxicity, the liposomal formulation was also tested in HT-29 cells, which do not secrete $sPLA_2$ (Fig. 7b). In this case, the liposomal formulation behaved similarly to the free C_{16}-MTX-ester, supporting our interpretation that the liposome formulated C_{16}-MTX-ester is available for cell uptake even without $sPLA_2$ hydrolysis, as the formulation would otherwise be nontoxic to the cells. Noteworthy though, the liposomal formulation proved more toxic than pure C_{16}-MTX-ester when $sPLA_2$ was added externally in the form of COLO 205 conditioned media. At first glance, this observation may seem contradictory and suggest a $sPLA_2$ dependent release of the MTX-derivative. However, the enhanced cytotoxicity at higher concentrations can be explained by the formation of lysolipid and fatty acid hydrolysis products, which are known to be cytotoxic in this concentration range (Jensen et al., 2004; Kim et al., 2007). In addition, the hydrolysis products may act as permeability enhancers that increase the toxicity of C_{16}-MTX-ester (Noseda et al., 1989; Davidsen et al., 2002), meaning that the increased cytotoxicity may well be unrelated to the release of C_{16}-MTX-ester. For these reasons, a more likely interpretation of the data would be that the C_{16}-MTX-ester is not adequately anchored in the liposomes, resulting in the dynamic partitioning of C_{16}-MTX-ester in and out of the liposomes. In this case, C_{16}-MTX-ester is available for cell uptake during the time it is present as a monomer in solution, and the cytotoxicity would resemble that of free MTX in accordance with our observations.

4.5. Anchoring stability

In order to test the hypothesis that the C16-MTX-ester was not adequately anchored in the liposomes, a simple DSC method was employed. The method is based on the addition of multilamellar liposomes as internal sensors that mimic the cancer cells in the cytotoxicity experiments (Fig. 8). After incubation for a specified time period, the extent of migration of MTX-ester from the liposomal formulation and into the multilamellar sensor liposomes can be assessed by recording a DSC scan and evaluating the perturbation of the main phase transition created by the MTX-ester. The results demonstrated that the DSC method was highly useful in assessing the anchoring stability of alkylated compounds, and showed that the MTX-ester was indeed only loosely anchored in the tested DPPC:DPPG:DPPE-PEG_{2000} (45:45:5:5) liposomes, as this formulation resulted in a significantly perturbed main phase transition peak of the DMPC sensor liposomes after incubation at 37 °C (see Fig. 9a). Using the DSC method it was also shown that the MTX-ester is particularly prone to dissociating from the liposomal formulation as the content of the negatively charged DPPG lipid increases (Fig. 10). Unfortunately, negatively charged lipids are necessary in order for the liposomes to be hydrolysable by $sPLA_2$, and removing the negatively charged lipids from the formulation is therefore not an option when designing liposomes for tumor specific release by $sPLA_2$. In future studies it would be logical to attempt to increase the anchoring stability by attaching either a longer alkyl chain or a double alkyl chain to MTX.

5. Conclusion

In this study, the synthesis of two lipophilic MTX-analogues has been described and their potential for liposomal tumor specific drug delivery has been evaluated. One analogue was found to be nontoxic, while the other analogue retained the full toxicity of the parent drug. This analogue was incorporated into liposomes that were designed to be particularly degradable by human $sPLA_2$. The potential benefits of this design are twofold. First of all, the liposomal carrier lipids are specifically hydrolyzed in cancer tissue that overexpress $sPLA_2$, resulting in a tumor specific release of the MTX-derivative. Secondly, the lysolipids and fatty acids that are the reaction products of the hydrolysis can act as permeability enhancers on cell membranes, which may increase the passive diffusion of the MTX-ester into cancer cells. The initial studies concerning the cytotoxicity, liposome incorporation, and PLA_2-mediated liposome degradation were highly promising, and demonstrated that it was possible to incorporate a cytotoxic C_{16}-MTX-ester analogue into $sPLA_2$-degradable liposomes. However, the cytotoxic activity results as well as a useful DSC method for evaluating the liposomal anchoring stability of alkylated compounds indicated that the MTX-derivative leaves the liposomes even in the absence of $sPLA_2$ hydrolysis. Future work is therefore needed to optimize the anchoring of the MTX-derivative in a liposomal formulation. However, the possibility of using fatty acid derivatized MTX-esters have been proven viable and it should be possible to

anchor the MTX-esters more tightly to the liposomal membrane by increasing the length of the hydrophobic chain.

Acknowledgment

MEMPHYS Center for Biomembrane Physics is supported by a grant from the Danish National Research Foundation.

References

Abe, T., Sakamoto, K., Kamohara, H., Hirano, Y., Kuwahara, N., Ogawa, M., 1997. Group II phospholipase A2 is increased in peritoneal and pleural effusions in patients with various types of cancer. Int. J. Cancer 74, 245–250.

Acute Leukemia Group B, 1965. New treatment schedule with improved survival in childhood leukemia. JAMA 194, 75–81.

Andresen, T.L., Jensen, S.S., Kaasgaard, T., Jørgensen, K., 2005. Triggered activation and release of liposomal prodrugs and drugs in cancer tissue by secretory phospholipase A2. Curr. Drug Deliv. 2, 353–362.

Bertino, J.R., Goker, E., Gorlick, R., Li, W.W., Banerjee, D., 1996. Resistance mechanisms to methotrexate in tumors. Stem Cells 14, 5–9.

Biltonen, R.L., Lichtenberg, D., 1993. The use of differential scanning calorimetry as a tool to characterize liposome preparations. Chem. Phys. Lipids 64, 129–142.

Buckland, A.G., Heeley, E.L., Wilton, D.C., 2000. Bacterial cell membrane hydrolysis by secreted phospholipases A(2): a major physiological role of human group IIa sPLA(2) involving both bacterial cell wall penetration and interfacial catalysis. Biochim. Biophys. Acta 1484, 195–206.

Buckland, A.G., Wilton, D.C., 2000. Anionic phospholipids, interfacial binding and the regulation of cell functions. Biochim. Biophys. Acta 1483, 199–216.

Carmichael, J., DeGraff, W.G., Gazdar, A.F., Minna, J.D., Mitchell, J.B., 1987. Evaluation of a tetrazolium-based semiautomated colorimetric assay: assessment of chemosensitivity testing. Cancer Res. 47, 936–942.

Davidsen, J., Mouritsen, O.G., Jørgensen, K., 2002. Synergistic permeability enhancing effect of lysophospholipids and fatty acids on lipid membranes. Biochim. Biophys. Acta 1564, 256–262.

Frei III, E., Rosowsky, A., Wright, J.E., Cucchi, C.A., Lippke, J.A., Ervin, T.J., Jolivet, J., Haseltine, W.A., 1984. Development of methotrexate resistance in human squamous cell carcinoma of the head and neck in culture. Proc. Natl. Acad. Sci. U.S.A. 81, 2873–2877.

Graff, J.R., Konicek, B.W., Deddens, J.A., Chedid, M., Hurst, B.M., Colligan, B., Neubauer, B.L., Carter, H.W., Carter, J.H., 2001. Expression of group IIa secretory phospholipase A2 increases with prostate tumor grade. Clin. Cancer Res. 7, 3857–3861.

Hønger, T., Jørgensen, K., Biltonen, R.L., Mouritsen, O.G., 1996. Systematic relationship between phospholipase A(2) activity and dynamic lipid bilayer microheterogeneity. Biochemistry 35, 9003–9006.

Høyrup, P., Callisen, T.H., Jensen, M.Ø., Halperin, A., Mouritsen, O.G., 2004. Lipid protrusions, membrane softness, and enzymatic activity. Phys. Chem. Chem. Phys. 6, 1608–1615.

Jensen, S.S., Andresen, T.L., Davidsen, J., Høyrup, P., Shnyder, S.D., Bibby, M.C., Gill, J.H., Jørgensen, K., 2004. Secretory phospholipase A2 as a tumor-specific trigger for targeted delivery of a novel class of liposomal prodrug anticancer etherlipids. Mol. Cancer Ther. 3, 1451–1458.

Jiang, J., Neubauer, B.L., Graff, J.R., Chedid, M., Thomas, J.E., Roehm, N.W., Zhang, S., Eckert, G.J., Koch, M.O., Eble, J.N., Cheng, L., 2002. Expression of group IIA secretory phospholipase A2 is elevated in prostatic intraepithelial neoplasia and adenocarcinoma. Am. J. Pathol. 160, 667–671.

Kim, Y.-L., Im, Y.-J., Ha, N.-C., Im, D.-S., 2007. Albumin inhibits cytotoxic activity of lysophosphatidylcholine by direct binding. Prostaglandins Other Lipid Mediat. 83, 130–138.

Leidy, C., Linderoth, L., Andresen, T.L., Mouritsen, O.G., Jørgensen, K., Peters, G.H., 2006. Domain-induced activation of human phospholipase A_2 Type IIA: local versus global lipid composition. Biophys. J. 90, 3165–3175.

Maraganore, J.M., Merutka, G., Cho, W., Welches, W., Kezdy, F.J., Heinrikson, R.L., 1984. A new class of phospholipases A2 with lysine in place of aspartate 49. Functional consequences for calcium binding and substrate binding. J. Biol. Chem. 259, 3839–3843.

Mauritz, R., Peters, G.J., Priest, D.G., Assaraf, Y.G., Drori, S., Kathmann, I., Noordhuis, P., Bunni, M.A., Rosowsky, A., Schornagel, J.H., Pinedo, H.M., Jansen, G., 2002. Multiple mechanisms of resistance to methotrexate and novel antifolates in human CCRF-CEM leukemia cells and their implications for folate homeostasis. Biochem. Pharmacol. 63, 105–115.

Montgomery, J.A., Piper, J.R., Elliott, R.D., Temple, C., Roberts, E.C., Shealy, Y.F., 1979. Analogues of methotrexate. J. Med. Chem. 22, 862–868.

Nayar, R., Hope, M.J., Cullis, P.R., 1989. Generation of large unilamellar vesicles from long-chain saturated phosphatidylcholines by extrusion technique. Biochim. Biophys. Acta 986, 200–206.

Noseda, A., White, J.G., Godwin, P.L., Jerome, W.G., Modest, E.J., 1989. Membrane damage in leukemic cells induced by ether and ester lipids: an electron microscopic study. Exp. Mol. Pathol. 50, 69–83.

Pignatello, R., Puleo, A., Puglisi, G., Vicari, L., Messina, A., 2003. Effect of liposomal delivery on in vitro antitumor activity of lipophilic conjugates of methotrexate with lipoamino acids. Drug Deliv. 10, 95–100.

Pignatello, R., Guccione, S., Forte, S., Di Giacomo, C., Sorrenti, V., Vicari, L., Barretta, G.U., Balzano, F., Puglisi, G., 2004. Lipophilic conjugates of methotrexate with short-chain alkylamino acids as DHFR inhibitors. Synthesis, biological evaluation, and molecular modelling. Bioorg. Med. Chem. 12, 2951–2964.

Piper, J.R., McCaleb, G.S., Montgomery, J.A., Kisliuk, R.L., Gaumont, Y., Sirotnak, F.M., 1982a. 10-Propargylaminopterin and alkyl homologs of methotrexate as inhibitors of folate metabolism. J. Med. Chem. 25, 877–880.

Piper, J.R., Montgomery, J.A., Sirotnak, F.M., Chello, P.L., 1982b. Synthesis of alpha-substituted and gamma-substituted amides, peptides, and esters of methotrexate and their evaluation as inhibitors of folate metabolism. J. Med. Chem. 25, 182–187.

Qu, X.D., Lehrer, R.I., 1998. Secretory phospholipase A2 is the principal bactericide for staphylococci and other Gram-positive bacteria in human tears. Infect. Immun. 66, 2791–2797.

Rosowsky, A., Forsch, R.A., Uren, J., Wick, M., 1981. Methotrexate analogues. 14. Synthesis of new gamma-substituted derivatives as dihydrofolate reductase inhibitors and potential anticancer agents. J. Med. Chem. 24, 1450–1455.

Rosowsky, A., Forsch, R., Uren, J., Wick, M., Kumar, A.A., Freisheim, J.H., 1983. Methotrexate analogues. 20. Replacement of glutamate by longer-chain amino diacids: effects on dihydrofolate reductase inhibition, cytotoxicity, and in vivo antitumor activity. J. Med. Chem. 26, 1719–1724.

Rosowsky, A., Forsch, R.A., Yu, C.-S., Lazarus, H., Beardsley, G.P., 1984. Methotrexate analogues. 21. Divergent influence of alkyl chain length on the dihydrofolate reductase affinity and cytotoxicity of methotrexate monoesters. J. Med. Chem. 27, 605–609.

Rosowsky, A., Bader, H., Radike-Smith, M., Cucchi, C.A., Wick, M.M., Freisheim, J.H., 1986. Methotrexate analogues. 28. Synthesis and biological evaluation of new gamma-monoamides of aminopterin and methotrexate. J. Med. Chem. 29, 1703–1709.

Rosowsky, A., Bader, H., Forsch, R.A., Moran, R.G., Freisheim, J.H., 1988a. Methotrexate analogues. 31. Meta and ortho isomers of aminopterin, compounds with a double bond in the side chain, and a novel analogue modified at the alpha-carbon: chemical and in vitro biological studies. J. Med. Chem. 31, 763–768.

Rosowsky, A., Forsch, R.A., Moran, R.G., Kohler, W., Freisheim, J.H., 1988b. Methotrexate analogues. 32. Chain extension, alpha-carboxyl deletion, and gamma-carboxyl replacement by sulfonate and phosphonate: effect on enzyme binding and cell-growth inhibition. J. Med. Chem. 31, 1326–1331.

Serra, M., Reverter-Branch, G., Maurici, D., Benini, S., Shen, J.N., Chano, T., Hattinger, C.M., Manara, M.C., Pasello, M., Scotlandi, K., Picci, P., 2004. Analysis of dihydrofolate reductase and reduced folate carrier gene status in relation to methotrexate resistance in osteosarcoma cells. Ann. Oncol. 15, 151–160.

Subramanian, S., Kaufman, B.T., 1978. Interaction of methotrexate, folates, and pyridine nucleotides with dihydrofolate reductase: calorimetric and spectroscopic binding studies. Proc. Natl. Acad. Sci. U.S.A. 75, 3201–3205.

Tenchov, B., 1991. On the reversibility of the phase-transitions in lipid-water systems. Chem. Phys. Lipids 57, 165–177.

Zerouga, M., Stillwell, W., Jenski, L.J., 2002. Synthesis of a novel phosphatidylcholine conjugated to docosahexaenoic acid and methotrexate that inhibits cell proliferation. Anti-Cancer Drugs 13, 301–311.